# Adaptive neural control for self-organized locomotion and obstacle negotiation of quadruped robots

T. Sun, D. Shao, Z. Dai*, and P. Manoonpong*

***Abstract*—Many quadruped robots have been developed to imitate their biological counterparts, several of which show excellent performance. However, the biological neural control mechanisms responsible for self-organized adaptive quadruped locomotion remain elusive. By drawing lessons from biological findings and using an artificial neural approach, we simulated a mammal-like quadruped robot and used it as our simulation platform to investigate and develop neural control mechanisms. In this study, we proposed an adaptive neural control network that can autonomously generate self-organized emergent locomotion with adaptability for the robot. The control network consists of three main components: Decoupled neural central pattern generator circuits (one for each leg), sensory feedback adaptation with dual-rate learning, and multiple neural reflex mechanisms. Simulation results show that the robot can perform quadruped-like gaits in a self-organized manner and adapt its gait to negotiate an obstacle. In addition, this work also suggests that the tight combination of the body-environment interaction and adaptive neural control, guided by sensory feedback adaptation and neural reflexes, is a powerful approach to better understand and solve self-organized adaptive coordination problems in quadruped locomotion.**

**Keywords**: Adaptive neural control, Reflexes, Central pattern generator, Self-organized locomotion, Quadruped.

## I. Introduction

Quadruped animals exhibit versatile locomotion patterns in response to the walking speed and environmental situations [1]. Many quadruped robots have been developed to imitate their biological counterparts. Several of them exhibit excellent performance [2-6]. For example, Boston Dynamics (BD) has released several impressively versatile quadruped robots since 2004 and 2007. The robots include BigDog, LS3, Wildcat, Spot and SpotMini[1]. These robots employ an engineering control approach based on state machine, dynamic balancing, foot trajectory planning and virtual leg methods [7] with predefined leg coordination. Although the control approach allows the robot to deal with terrain changes through terrain sensing and posture control [3], it is difficult to relate the approach to its biological counterpart as well as to better understand and solve self-organized adaptive coordination problems in quadruped locomotion.

In contrast to the engineering control approach, biological findings have revealed that the locomotion of quadruped animals is basically generated by a combination of central pattern generators (CPGs), sensory feedback, and reflexes [8, 9]. Inspired by the findings, various bio-inspired control approaches of quadruped robots have been developed [10-14]. For example, Fukuoka and Kimura introduced a control network with four CPGs and reflex mechanisms to allow the robot Tekken to walk on uneven terrain [10]. Nevertheless, this bio-inspired CPG- and reflex-based control method requires preprogrammed phase relationships between CPGs. Thereby, it lacks in flexibility, independency, and self-organization properties.

To overcome the problems, Owaki et al. presented alternative approach based on decoupled simple CPGs with continuous phase modulation [12]. Instead of predefining the CPG phase relationships, they modulated the CPG phases with respect to the magnitude of leg load sensing. This results in flexibility and adaptability to deal with the changes of weight distribution and locomotion speed of a quadruped robot. While this method can generate self-organized locomotion, the load sensing feedback gain, which is an important factor to properly modulate the CPG phases and, thereby, achieve stable locomotion, has been manually adjusted. Furthermore, the approach has not been applied or investigated on gait adaptation to negotiate an obstacle, which is a specific practical situation for robots when walking in a natural environment. Although some researches have proposed reflex mechanisms for negotiating obstacles [2, 3, 13, 14], e.g. Focchi et al. (2013) presented reflex generation for obstacle negotiation through a kinematic modification of the reference trajectory [13], their approaches do not include self-organized locomotion which can provide more flexibility and adaptability to deal with uneven terrain. CPGs, reflexes, and sensory feedback observed in animals have been a major source inspiration for adaptive locomotion control of quadruped robots in many researches [9-13]. The majority of CPG and reflex models, under appropriate adjustments of sensory feedback, have been applied to enable robots to adapt to changes of irregularity terrain. However, not all models are available for exploiting decoupled CPGs to form self-organized locomotion.

From this point of view, in this study, we proposed adaptive neural control based on decoupled CPGs with sensory feedback adaptation and neural reflexes for self-organized locomotion and obstacle negotiation. Our approach, inspired by [2, 12, 16], has the following distinguished aspects: 1) decoupled neural CPG circuits for flexible and independent individual leg control, 2) sensory feedback adaptation with dual-rate learning for automatic feedback gain adjustment and generalization, and 3) neural reflex mechanisms for stability and obstacle negotiation. This results in self-organized interlimb coordination allowing our simulated mammal-like quadruped robot to adaptively form quadruped-like gaits and negotiate an obstacle.

T. Sun, D. Shao, and *Z Dai are with Institute of Bio-inspired Structure and Surface Engineering, Nanjing University of Aeronautics and Astronautics, 29 Yudao Street, Nanjing 210016, PR China (e-mail: suntao.hn@qq.com).

*P. Manoonpong is with Institute of Bio-inspired Structure and Surface Engineering, Nanjing University of Aeronautics and Astronautics, 29 Yudao Street, Nanjing 210016, PR China and Embodied AI & Neurobotics Lab, Centre for BioRobotics, The Mærsk Mc-Kinney Møller Institute, The University of Southern Denmark, Odense M, DK-5230, Denmark (e-mail: poma@nuaa.edu.cn).

[1] https://www.bostondynamics.com/

Our contribution is a self-organized quadrupedal locomotion generator based on adaptive neural control with decoupled CPG circuits, sensory feedback adaptation and neural reflex mechanisms. Another key contribution of this work is an implementation of dual-rate learning to tune feedback gains online.

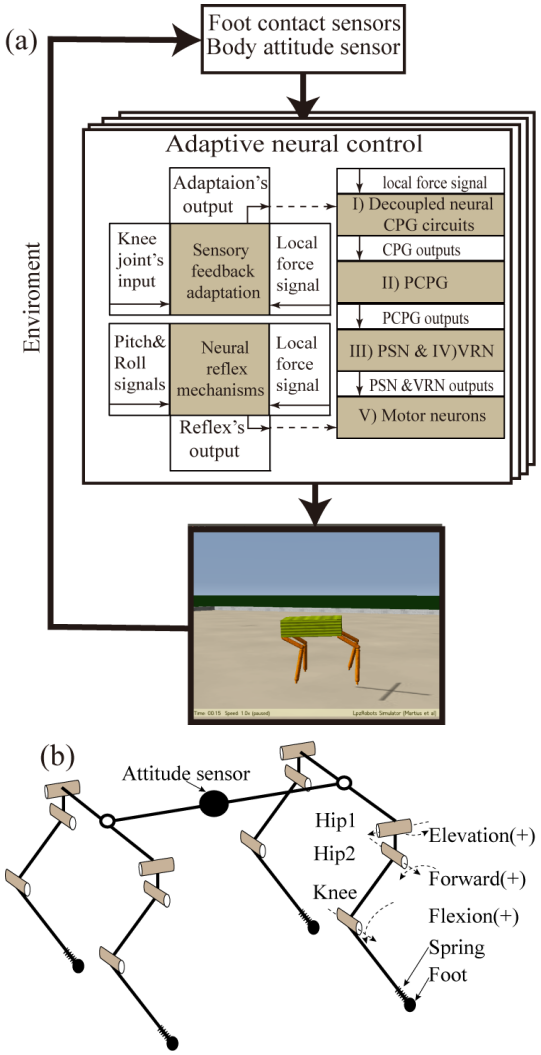


Figure 1. (a) The overview diagram of the adaptive neural control embedded in the sensorimotor loop. The control consists of three main mechanisms: Decoupled neural CPG circuits, sensory feedback adaptation, and neural reflex mechanisms. (b) Mechanical setup of the robot in this study

## II. System Overview

In this study, self-organized locomotion and obstacle negotiation of a quadruped robot are achieved via a sensorimotor loop which involves adaptive neural control, sensory feedback, and robot body dynamics (Fig. 1(a)). The adaptive neural control has three main mechanisms: Decoupled neural CPG circuits, sensory feedback adaptation with dual-rate learning, and neural reflex mechanisms (described in the section below). Here we simulated a mammal-like quadruped robot using the Modular Robot Control Environment embedded in the LpzRobots toolkit [17]. It was used for developing and testing our neural control. The morphology and dimensions of the robot were modelled based on the Laikago dog robot of UNITREE[2]. It has four identical legs. Each leg has three joints (Fig. 1(b)). The hip1 joint enables elevation (+) and depression (-) of the thigh, the hip2 joint enables forward (+) and backward (-) movements, and the knee joint enables flexion (+) and extension (-) of the calf. Each leg contains a spring compliant element of the foot to substitute tendon and muscle viscoelasticity. We also implemented a foot contact sensor on each leg and a 2-axis body attitude sensor (roll, pitch). It has dimensions of 560 mm × 350 mm × 160 mm, while the lengths of the thigh and calf are 200 mm and 275 mm, respectively (see in Fig. 1(b)). The mass of the whole robot is 28.2 kg.

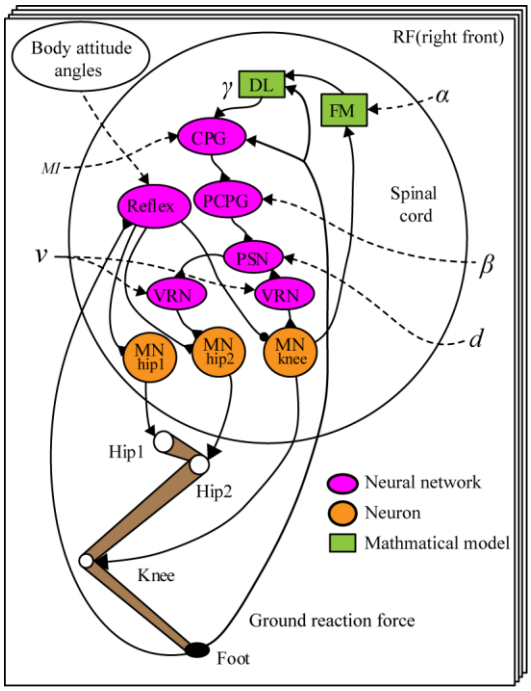


Figure 2. The detail diagram of the identical adaptive neural control of four legs: right front (RF), right hind (RH), left front (LF) and left hind (LH), respectively. It consists of a decoupled neural CPG circuit with five subnetworks or modules including (central pattern generator) CPG, (postprocessing PCPG) PCPG, (phase switching network) PSN, (velocity regulating network) VRN and (motor neurons) MNs, sensory feedback adaptation with a forward model (FM) and a dual-rate learning algorithm(DL), and neural reflexes generating commands to motor neurons responding to the changes of body attitude signals. The performance of the adaptive neural control network can be adjusted by five parameters: $\alpha$, $\beta$, $d$, $\nu$ and $MI$. The functionalities of the parameters are described as follows: $\alpha$ can adjust the amplitude of the FM output, $\beta$ is able to indirectly decide the period of stance phase, $d$ can switch the phases of the PCPG outputs, $\nu$ can adjust the amplitude of the VRN output, $MI$ can adjust the frequencies of CPG signals. These parameters have been empirically set as: $\alpha = 0.55$, $\beta = 0.64$, $d = 1$, $\nu = 0.08$, $MI = 0.075$ in the following experiments (more details can be seen at [16]).

## III. Adaptive Neural Control for Self-Organized Locomotion and Obstacle Negotiation

### A. Decoupled neural CPG circuits

The decoupled neural CPG circuits play a pivotal role for inducing self-organized quadruped locomotion in this study. Here we have four identical CPG circuits. Each of them, controlling one leg, consists of five elements or modules (Fig.

[2] http://www.unitree.cc/

2): 1) neural oscillator network serving as a CPG for generating basic rhythmic patterns, 2) neural postprocessing of CPG (PCPG) for shaping CPG's output signals and, thereby, adjusting foot trajectory, 3) velocity regulating network (VRN) for regulating the hip2 joint signal, 4) phase switching network (PSN) for switching the phase of PCPG's outputs, 5) motor neurons (MNs) for transmitting motor commands to three leg joints of the robot.

As for the CPG, it generates two periodic output signals, which are provided to the hip2 joint and the knee joint only indirectly passing through PCPG, PSN, VRN, and MNs. Thus, the basic rhythmic leg movement is generated by the CPG. The smooth foot trajectory is achieved by PCPG in accordance with the given input $\beta$. The steering capability is realized by PSN and VRN in accordance with the given inputs $v$ and $d$. MNs are used to send control signals to motors. The detail descriptions of PSN and VRN can be seen at [16].

In detail, we use a CPG with sensory feedback proposed by [18]. It consists of two mutually inhibiting neurons (Fig. 2). Each neuron in this model is represented by the following equations:

$$\begin{aligned} a_1(n+1) &= \sum_{j=1}^{2} w_{1j} o_j(n) + B_1 - \gamma_1 F(n)\cos(a_1(n)), \\ a_2(n+1) &= \sum_{j=1}^{2} w_{2j} o_j(n) + B_2 - \gamma_2 F(n)\sin(a_2(n)), \\ o_j(n+1) &= \tanh(a_j(n+1)),\ j = 1, 2. \end{aligned} \tag{1}$$

$\gamma_{1,2}$ are positive variables as the sensory feedback gain automatically adjusted by dual-rate learning. It is described in detail in the following section. $F(n)$ represents the continuous ground reaction force (GRF) detected by the foot contact sensor (FC) as a sensory feedback to CPG. $B_{1,2}$ represent fixed internal bias terms of two neurons, $w_{1j,2j}$ are the synaptic weight of the connection from the $j$th neuron to the 1th and the 2th neuron. $a_i(n)$ is the neuron activity, and $o_i(n)$ is the neuron output. In these equations, $F(n) \approx 0$ if a foot does not touch the ground. The weight and bias parameters were empirically set as: $B_{1,2} = 0.01$, $w_{11,22} = 1.4$, $w_{12} = MI + 0.18$, $w_{21} = -MI - 0.18$, $MI = [0.04, 0.12]$ in order to realize intralimb coordination. $MI$ can adjust the frequencies of CPG signals. The detailed description of the parameters is referred to [16].

PCPG can smooth the outputs of CPG. It is represented by the following equations:

$$\begin{aligned} a^{P}_{1,2}(n) &= \begin{cases} 1, o_{1,2}(n) >= \beta \\ -1, o_{1,2}(n) < \beta \end{cases}, \\ b(n) &= \begin{cases} 1, a^{P}_{1,2}(n) = 1 \\ -1, a^{P}_{1,2}(n) = -1 \end{cases}, \\ k(n) &= \begin{cases} 2/N, a^{P}_{1,2}(n) = 1 \\ -2/N, k_2, a^{P}_{1,2}(n) = -1 \end{cases}, \\ N &= \max(n), \\ o^{P}_{1,2}(n) &= k(n) * n + b(n), n = 0, 1, ..N. \end{aligned} \tag{2}$$

$o_{1,2}(n)$ are the CPG outputs, $\beta$ is a variable to adjust the raising period of output signals. $a^{P}_{1,2}(n)$ are PCPG's activities. $o^{P}_{1,2}(n)$ are its outputs corresponding to the inputs, that are linear with step $n$, and $b(n)$ and $k(n)$ are the slope and intercept of this linear relationship, respectively. In these equations, the output ascends from -1 to 1 if the input is greater than $\beta$ ($o(n) \geq \beta$). The output descends from 1 to -1 if the input is less than $\beta$ ($o(n) < \beta$). Thus, the periods of the flexion and extension movements of the knee joint can be modified by $\beta$ to indirectly modulate the duty factor of foot trajectory.

MNs include three motor neurons corresponding to three joints of one leg. All motor neurons are modelled as discrete-time non-spiking neurons. They collect command signals from the CPG based control network and the reflex network, and then drive the joint motors of one leg. The activity and output of each neuron are governed by following equations:

$$\begin{aligned} a_i(n+1) &= \sum_{j=1}^{n} w_{ij} o_j(n) + B_i, \\ o_i(n+1) &= \tanh(a_i(n+1)), i = 1, 2, 3. \end{aligned} \tag{3}$$

$o_j(n)$ is an input coming from PSN or VRN and reflex (described in subsection C). $n$ denotes the number of neurons connected to the motor neurons, while $i$ indicates a motor neuron. $B_i$ is the bias term of a motor neuron, $a_i(n)$ is the activity, and $o_i(n)$ is the output.

### *B. Sensory feedback adaptation with dual-rate learning*

The suitable sensory feedback gains $\gamma_{1,2}$ play an important role to properly modulate the CPG phases and, thereby, form self-organized stable locomotion. To automatically adjust the gains and, hence, online tune this decoupled CPG circuits, we applied a dual-rate based learning mechanism [20] (Fig. 2, green blocks). There are two components underlying the learning mechanism: 1) a two-rate, gain-independent learning algorithm (DL), inspired by [21], and 2) a forward model (FM). DL uses the error signal, i.e., the difference between an expected ground reaction force (GRF) and a real GRF, to output the sensory feedback gains. FM is used here to translate the output of the knee motor neuron into the expected GRF for the learning algorithm. FM uses the following equations for the translation:

$$\begin{aligned} F^{e}(n+1) &= \alpha(\rho G(n) + (1 - \rho) F^{e}(n)), \\ G(n) &= \begin{cases} 1, \theta_2(n) <= \theta_2(n-1) \\ 0, \theta_2(n) > \theta_2(n-1) \end{cases}. \end{aligned} \tag{4}$$

$\theta_2(n)$ is the output of the motor neuron of the knee joint, $F^{e}(n+1)$ is the expected GRF, and $\rho$ is a shaping parameter for the expected GRF. It has a range of [0, 1], we found that $\rho = 0.99$ is easier to make the expected GRF similar to real GRF through simulation test. $\alpha$ is a scaling factor to scale the amplitude of the expected GRF such that it matches the real GRF. $G(n)$ is a variable for switching expected stance phase and swing phase depending on the $\theta_2(n)$. In the following experiments, the parameters were set to $\alpha = 0.55$.

To reduce the difference, this learning process consists of a fast learner and a slow learner, both are modelled as linear systems that act in parallel. The dual rate learner follows the equations:

$$
\begin{aligned}
&e(n) = F^{r}(n) - F^{e}(n),\\
&K_f(n+1) = A_f K_f(n) + B_f e(n),\\
&K_s(n+1) = A_s K_s(n) + B_s e(n),\\
&\gamma_1(n) = K(K_f(n) + K_s(n)) + M,\\
&\gamma_2(n) = \gamma_1(n) + 0.005.
\end{aligned}
\qquad (5)
$$

$F^r(n)$ and $F^e(n)$ are real GRF and expected GRF, respectively. $B_s$ and $B_f$ correspond to the learning rate of the slow and fast learners. $A_s$ and $A_f$ are two retention factors. The fast and slow learners can be differentiated by these parameters. The fast learner has a higher learning rate, where the slow learner is characterized by a high retention rate, being necessary that $A_s > A_f$ and $B_s < B_f$. $K$ is a global scaling factor, and M is a global retention factor. The parameters of the learning used in this paper have been empirically set as: $A_s$ = 0.993, $A_f$ = 0.57, $B_s$ = 0.0002, $B_f$ = 0.002, $K$ = 10, $M$ = 0.08, the detail information can be seen in [19].

### C. Neural reflex mechanisms

In order to improve the attitude stability of the robot so that it can negotiate obstacle during locomotion, attitude control of the reflex mechanism has been implemented by drawing lessons from biological performing concepts [22, 23]: When the vestibule in a head detects an inclination in pitch or roll plane, a downward-inclined leg is extended while an upward-inclined leg is flexed (Fig. 3).

A neural network implementing the reflex mechanisms was developed by imitating the biological behaviors to achieve the attitude control (Fig. 3(b)). As shown in Fig. 3(b), the network contained three components: three input neurons, a VRN, and two output neurons. The input neurons N1 and N2 receive body attitude information and N3 receives local real GRF information. In detail, a recurrent connection has been implemented on N1 to calculate the derivation of the attitude signals. N2 receives and then sums the derivation term of the attitude signals from N1 and the original term of the attitude sensor. The outputs of N2 and N3 are multiplied by VRN, which enable the stance legs to generate response except for swing legs. The N4 and N5 neurons are connected to the motor neurons of the hip2 joint and the knee joint, respectively. $w_{1r,2r}$ are the synaptic weights between the body roll and N1 and N2. $w_{1P,2P}$ are the synaptic weights between the body pitch and N1 and N2. All neurons of this network are modelled as discrete-time non-spiking neurons. The transfer functions of these neurons are a hyperbolic tangent function except for N4 and N5 whose are a linear function.

In addition, the corrective reflex behaviors of four legs depend heavily on the synaptic weights. For example, $w_{1r}$ of ipsilateral legs have same sign, whereas contralateral legs are opposite sign. Moreover, $w_{1P}$ is the same for the fore and rear legs (see Fig. 3(c)). As for the values of the synaptic weights, they just depend on the lengths of calf and thigh as well as the power of actuator of the specific robot. We set these values for our simulated robot through empirical tests. The resulting synaptic weights are as shown in Fig. 3(c).

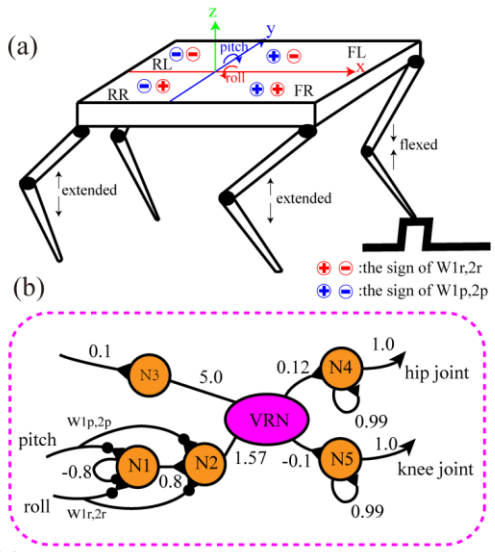


(c)

| Leg | $w_{1r,2r}$ | $w_{1p,2p}$ |
|---|---|---|
| RF | 0.7 | 0.8 |
| RH | 0.7 | -0.8 |
| LF | -0.7 | 0.8 |
| LH | -0.7 | -0.8 |

Figure 3. Neural reflex mechanisms. Reflex behaviors with respect to pitch and roll signals of the robot body.

## IV. Simulation Results

To evaluate the performance of the proposed adaptive neural control, two simulations were carried out (Fig. 4). The first one was to explore the performance of self-organized adaptive locomotion of the simulated robots on flat terrain (see Fig. 5). The second one was to compare the robot's attitude stability (roll, pitch) between the decoupled neural CPG circuits with and without the neural reflex mechanisms while negotiating an obstacle. The obstacle height is about one third of the calf length of the robot (see Figs. 6). The neural control parameters for our experiments are listed in Table 1.

As shown in Fig. 5, we initiated the decoupled neural CPG circuits to outputs in phase while the robot was fixed in the air at beginning. As soon as the robot was dropped on the ground at around 5 s, the sensory feedback mechanisms were enabled. The gains of the sensory feedback were automatically adjusted. After around 8 s, the gains were converted and oscillated around 0.15. As a consequence, a walk gait autonomously emerged. This gait is the transversal gait between tort and pace gaits [10]. From the simulation results, one can see that such a quadruped-like gait was generated in a self-organized manner. This was induced by decoupled neural CPG circuits with sensory feedback adaptation after a short period of time.

As shown in Fig. 6, the robot walked forward to negotiate an obstacle using two compared control approaches, decoupled neural CPG circuits without and with neural reflex mechanisms. The walking process of the robot was divided into five stages (S1: the robot was fixed in the air, S2: the robot adapted its gait from irregular to regular, S3: the robot went forward with a walk gait, S4: the robot climbed the obstacle, S5: the robot crossed over the obstacle). Both

approaches almost induced same performance in robot's attitude stability and walking displacement from S1 to S3. Nevertheless, the robot using the first approach shows worse performance at the later walking stages. For instance, without the reflex mechanisms at S5, the forward displacement of the robot stalled in around 1.5 m (Fig. 6(a)), its gait was also disturbed (Fig. 6(b)), the pitch angle of the robot had bigger fluctuating (Fig. 6(d)). The reason of these is the robot got stuck on the obstacle and unable to walk down it at S4. As demonstrated, the robot based on the decoupled neural CPG circuits with sensory feedback adaptation and additional neural reflex mechanisms can show better walking performance while it negotiating an obstacle.

TABLE 1. RANGE AND VALUES OF THE PARAMETERS USED IN ALL EXPERIMENTS

| Parameter | Range | Value | Parameters | Range | Value |
|---|---|---|---|---|---|
| $\alpha$ | [0.0, 1.0] | 0.55 | $d$ | [-1.0, 1.0] | 1.0 |
| $\beta$ | [-0.8, 0.8] | 0.64 | $v$ | [-0.5, 0.5] | 0.08 |
| $MI$ | [0.04, 0.12] | 0.075 | | | |

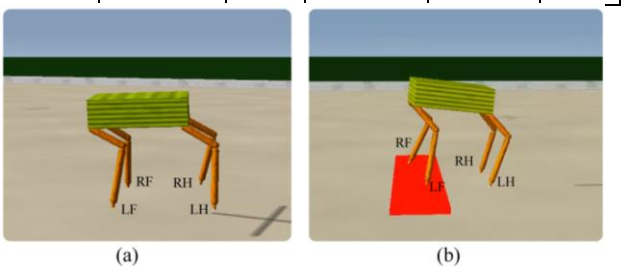


Figure 4. Simulation screenshots. (a) Self-organized quadruped locomotion on flat terrain. (b) Adaptive obstacle negotiation.

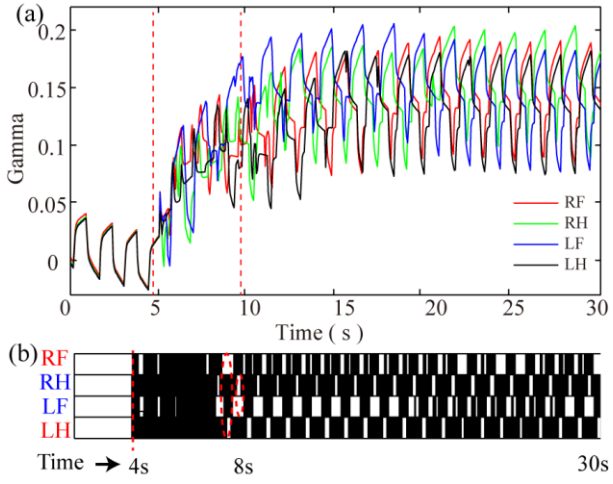


Figure 5. The process of generating a walk gait from initial state where all legs move in phase. (a) The snesory feedback gains of four identical legs. (b) The gait diagram from initialization (all the legs moved in same phase) to self-organized stable locomotion. The black areas indicate ground contact or stance phase. The white areas refer to no ground contact or swing phase. At the beginning, the robot was positioned in the air and then dropped on the ground at around 4 s. After around 8 s, a stable gait emerges. For this gait, the dignoal legs almost move in phase.Note that, RF is the right front leg, RH is the right hind leg, LF is the left front leg, and LH is the left hind leg. The video clip of this experiment can be seen at http://www.manoonpong.com/ROMAN2018/video1.mp4.

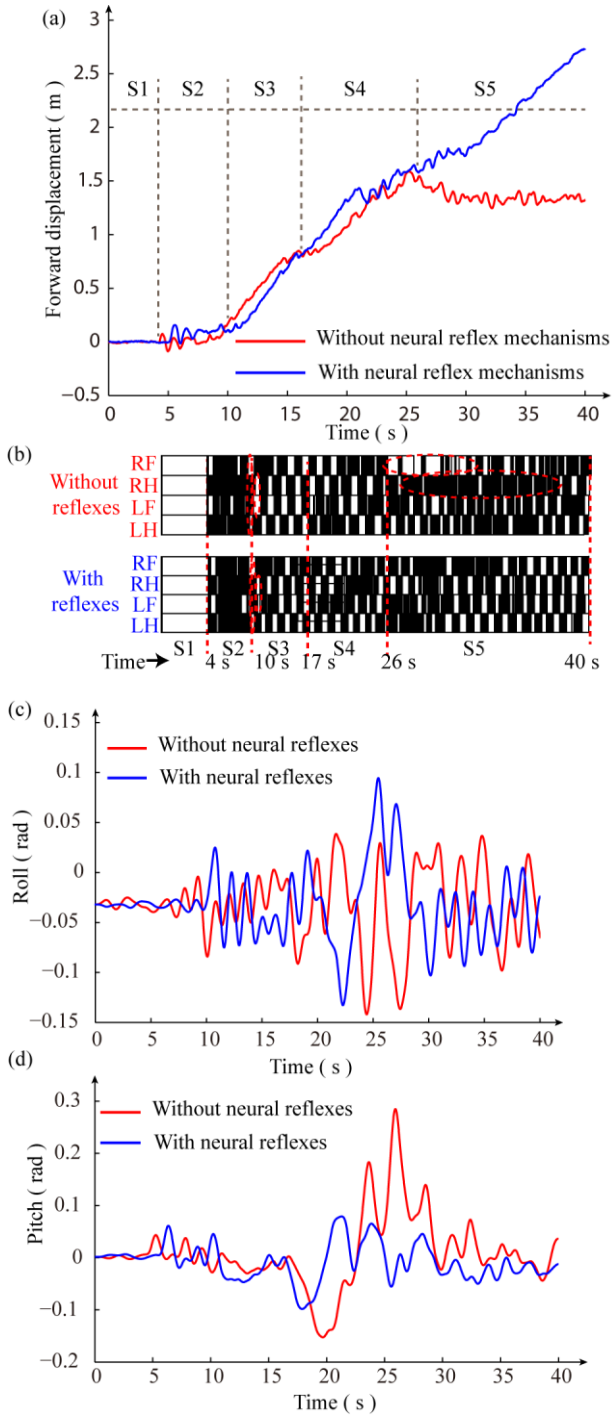


Figure 6. The robot negotiates an obstacle. The decoupled CPG circuits with and without the neural reflex mechanisms were used to test and compare. (a) The forward displacement of the robot from the two methods. The walking process was divided into five stages (S1: the robot was fixed in the air, S2: the robot adapted its gait from irregular to regular, S3: the robot went forward with a walk gait, S4: the robot climbed the obstacle, S5: the robot crossed over the obstacle). (b) The gait diagram of the robot from the two methods (The black areas indicate ground contact or stance phase, the white areas refer to no ground contact during swing phase). (c) The roll angles of the robot body under the two methods. (d) The pitch angles of the robot under the two methods. The video clip of this experiment can be seen at http://www.manoonpong.com/ROMAN2018/video2.mp4.

## V. Discussion and Conclusion

In this study, a mammal-like quadruped robot was presented to serve as a platform for developing and testing adaptive neural control for self-organized locomotion and obstacle negotiation. The simulation results demonstrate the capabilities of our control strategy in terms of self-organization, adaptation, and stability.

The contributions of this work include: self-organized quadruped locomotion on flat terrain generated by decoupled neural CPG circuits with sensory feedback adaptation. Each neural CPG circuits consists of five modules: CPG, PCPG, VRN, PSN, and MNs. As a result, the decoupled neural CPG circuits with sensory feedback adaptation can autonomously generate emergent quadruped locomotion. Additionally, with neural reflex mechanisms having three components (three input neurons, a VRN network, and two output neurons), the robot can adapt its self-organized gait to negotiate an obstacle. Furthermore, the structure of this adaptive neural control is independent of mechanical setup of a robot, it can be generally applied to other legged robots with only few parameter adjustment (i. e., $\alpha$, $\beta$).

Take together, this work suggests that a tight combination of the body-environment interaction and the adaptive neural control, guided sensory feedback adaptation and reflexes, is a powerful approach to better understand and solve self-organized adaptive coordination problems in quadruped locomotion. In the future, we aim to integrate more proprioceptive sensory feedback (e.g., joint angles) and muscle models to achieve robust locomotion against leg damage and multiple obstacle negotiation as well as to allow for more complex and energy-efficient locomotion on different slopes and substrates.

## Acknowledgment

This research was supported by Thousand Talents program of China (P.M.) and the National Natural Science Foundation of China (Grant NO. 51435008 to Z.D).

## References

[1] D. F. Hoyt and C. R. Taylor, "Gait and the energetics of locomotion in horses," *Nature*, vol. 292, pp. 239 - 240, 1981.

[2] Y. Fukuoka and H. Kimura, "Dynamic locomotion of a biomorphic quadruped ‘Tekken’ robot using various gaits: walk, trot, free-gait and bound," *Applied Bionics and Biomechanics*, vol. 6, pp. 63-71, 2009.

[3] K. Izumi, R. Sato and K. Watanabe, "Generation of obstacle avoidance behaviors for quadruped robots using finite automaton," in 2008 SICE Annual Conference, Seoul, Korea, 2008.

[4] D. Wooden, M. Malchano and K. Blankespoor, "Autonomous navigation for BigDog," in IEEE International Conference on Robotics and Automation, Anchorage, Alaska, 2010.

[5] C. Semini, N. G. Tsagarakis, E. Guglielmino, M. Focchi, F. Cannella, and D. G. Caldwell, "Design of HyQ - a hydraulically and electrically actuated quadruped robot," *Proceedings of the Institution of Mechanical Engineers, Part I: Journal of Systems and Control Engineering*, vol. 225, pp. 831-849, 2011.

[6] C. Semini, V. Barasuol, J. Goldsmith, M. Frigerio, M. Focchi, Y. Gao, and D. G. Caldwell, "Design of the Hydraulically Actuated, Torque-Controlled Quadruped Robot HyQ2Max," *IEEE/ASME Transactions on Mechatronics*, vol. 22, pp. 635-646, 2017.

[7] M. H. Raibert, *Legged Robots That Balance*, Cambridge Massachusetts: The MIT Press, 1986.

[8] S. Grillner, "Control of Locomotion in Bipeds, Tetrapods, and Fish," *Handbook of physiology II american phtsiology cociety*, pp. 1179-1236, 1981.

[9] A. H. Cohen and D. L. Boothe, "Sensorimotor Interactions During Locomotion: Principles Derived from Biological Systems," *Autonomous Robots*, vol. 7, pp. 239-245, 1999.

[10] H. Kimura, Y. Fukuoka and A. H. Cohen, "Adaptive Dynamic Walking of a Quadruped Robot on Natural Ground Based on Biological Concepts," *The International Journal of Robotics Research*, vol. 5, pp. 475-490, 2007.

[11] D. T. Tran, I. M. Koo, Y. H. Lee, H. Moon, S. Park, J. C. Koo, and H. R. Choi, "Central pattern generator based reflexive control of quadruped walking robots using a recurrent neural network," *Robotics & Autonomous Systems*, vol. 62, pp. 1497-1516, 2014.

[12] D. Owaki, T. Kano, K. Nagasawa, A. Tero, and A. Ishiguro, "Simple robot suggests physical interlimb communication is essential for quadruped walking," *Journal of The Royal Society Interface*, vol. 10, 2013.

[13] M. Focchi, V. Barasuol, I. Havoutis, J. Buchli, C. Semini, and D. G. Caldwell, "Local reflex generation for obstacle negotiation in quadrupedal locomotion," in *Nature-Inspired Mobile Robotics*, ed: World Scientific, pp. 443-450, 2013.

[14] Z. Wang, C. Sun, G. Deng, and A. Zhang, "Locomotion planning for quadruped robot over rough terrain," *Chinese Automation Congress*, pp. 3170-3173, 2017.

[15] C. Liu, L. Xia, C. Zhang, and Q. Chen, "Multi-layered CPG for adaptive walking of quadruped robots," Journal of Bionic Engineering, vol. 15, pp. 341-355, 2018.

[16] P. Manoonpong, F. Pasemann and F. Wörgötter, "Sensor-driven neural control for omnidirectional locomotion and versatile reactive behaviors of walking machines," Robotics & Autonomous Systems, vol. 56, pp. 265-288, 2008.

[17] F. Hesse, G. Martius, P. Manoonpong, M. Biehl and F. Wörgötter, "Modular Robot Control Environment Testing Neural Control on Simulated and Real Robots," Frontiers in Computational Neuroscience, Conference Abstract, Bernstein Conference 2012, doi :10.3389/conf.fncom.2012.55.00179, 2012

[18] S. S. Barikhan, F. Wörgötter and P. Manoonpong, "Multiple Decoupled CPGs with Local Sensory Feedback for Adaptive Locomotion Behaviors of Bio-inspired Walking Robots," in *Springer International Publishing*, Cham, 2014, pp. 65-75.

[19] P. Manoonpong, U. Parlitz and F. Wörgötter, "Neural control and adaptive neural forward models for insect-like, energy-efficient, and adaptable locomotion of walking machines," *Frontiers in Neural Circuits*, vol. 7, 2013.

[20] A. M. Blanco, — locomotion control for complex behaviour of bio-inpsired multi-legged robotic systems, | M.S. thesis, Dept. Faculty of Engineering, University of Southern Denmark, Odense, Demark, 2017.

[21] M. A. Smith, A. Ghazizadeh and R. Shadmehr, "Interacting Adaptive Processes with Different Timescales Underlie Short-Term Motor Learning," *Plos Biology*, vol. 4, p. e179, 2006.

[22] Y. H. Kimura, "Adaptive dynamic walking of a quadruped robot on irregular terrain based on biological concepts," *The International Journal of Robotics Research*, vol. 3-4, pp. 187-202, 2003.

[23] A. A. Saputra, J. Botzheim, I. A. Sulistijono, N. Kubota, "Biologically Inspired Control System for 3-D Locomotion of a Humanoid Biped Robot," IEEE Transactions on Systems, Man, and Cybernetics: Systems, Vol. 46, No. 7, pp.898–911, 2016.